Synthesis, Characterization, and Solid-State Molecular Structures of Nitrosoarene Complexes of Osmium Porphyrins

Li Chen, Masood A. Khan, and George B. Richter-Addo*

Department of Chemistry and Biochemistry, University of Oklahoma, 620 Parrington Oval, Norman, Oklahoma 73019

Victor G. Young, Jr.

X-ray Structural Laboratory, Department of Chemistry, University of Minnesota, 207 Pleasant Street S.E., Minneapolis, Minnesota 55455

Douglas R. Powell

X-ray Structural Laboratory, Department of Chemistry, University of Wisconsin, 1101 University Avenue, Madison, Wisconsin 53706

The reactions of (por)Os(CO) (por = TPP, TTP, OEP, TMP) with nitrosoarenes (ArNO; Ar = Ph, *o*-tol) in refluxing toluene generate the (por)Os(ArNO)$_2$ complexes in 45−76% yields (TTP = 5,10,15,20-tetra-*p*-tolylporphyrinato dianion, TPP = 5,10,15,20-tetraphenylporphyrinato dianion, OEP = 2,3,7,8,12,13,17,18-octaethylporphyrinato dianion, TMP = 5,10,15,20-tetramesitylporphyrinato dianion). The ν_{NO} of the coordinated PhNO groups in the (por)Os(PhNO)$_2$ complexes occur in the 1295−1276 cm^{-1} range, and decrease slightly in the order TPP (1295 cm^{-1}) > TTP (1291 cm^{-1}) > OEP (1286 cm^{-1}) > TMP (1276 cm^{-1}). The reaction of (TTP)Os(CO) with 1 equiv of PhNO in CH$_2$Cl$_2$ at room temperature generates a 1:3 mixture of (TTP)Os(CO)(PhNO) and (TTP)Os(PhNO)$_2$ in ca. 40% isolated yield. The ν_{CO} of (TTP)Os(CO)(PhNO) is at 1972 cm^{-1} (KBr), which is 56 cm^{-1} *higher* in energy than that of the precursor (TTP)Os(CO). When this mixture and excess PhNO are dissolved in toluene and the solution is heated to reflux, quantitative conversion to the (TTP)Os(PhNO)$_2$ product occurs. IR monitoring of the reactions of (por)Os(CO) with 1 equiv of PhNO in CH$_2$Cl$_2$ reveal similar formations of the respective (por)Os(CO)(PhNO) intermediates for the TTP (1968 cm^{-1}; $\Delta\nu_{CO}$ = +74 cm^{-1}), TMP (1966 cm^{-1}; $\Delta\nu_{CO}$ = +63 cm^{-1}), and OEP (1958 cm^{-1}; $\Delta\nu_{CO}$ = +72 cm^{-1}) analogues. Five of these (por)Os(ArNO)-containing complexes have been fully characterized by spectroscopic methods and by single-crystal X-ray crystallography. All the nitrosoarene ligands in these complexes are attached to the formally Os^{II} centers via an η^1-N binding mode.

Introduction

The interest in the chemistry of nitrosoarenes (ArN=O; Ar = aryl) and nitrosoalkanes (RN=O; R = alkyl) is due partly to the observation that these *C*-nitroso compounds are known to bind to the metal centers in heme-containing biomolecules such as cytochrome P450,[1−7] hemoglobin,[8−12] myoglobin,[9] and guanylyl cyclase.[13] The structural and reaction chemistries of *C*-nitroso compounds have been the subject of numerous studies.[14−22]

The coordination chemistry of *C*-nitroso compounds has been reviewed.[23] In general, the nitroso functionality of *C*-nitroso

compounds may interact with monometallic metal centers in one of three ways (Chart 1).

All three modes have been characterized by single-crystal X-ray crystallography. Some examples of type **A** complexes include those of W and Fe.[24,25] Type **B** complexes are less common, with X-ray structural determinations obtained, for example, for monometallic complexes of W,[26] Pt,[27] Mo,[28−30] and Ru.[31,32] Structural reports on the related bimetallic μ-η^2:η^2

(1) Fukuto, J. M.; Brady, J. F.; Burstyn, J. N.; VanAtta, R. B.; Valentine, J. S.; Cho, A. K. *Biochemistry* **1986**, *25*, 2714−2719.
(2) Mansuy, D.; Gans, P.; Chottard, J.-C.; Bartoli, J.-F. *Eur. J. Biochem.* **1977**, *76*, 607−615.
(3) Mansuy, D.; Rouer, E.; Bacot, C.; Gans, P.; Chottard, J. C.; Leroux, J. P. *Biochem. Pharmacol.* **1978**, *27*, 1229−1237.
(4) Mansuy, D.; Beaune, P.; Chottard, J. C.; Bartoli, J. F.; Gans, P. *Biochem. Pharmacol.* **1976**, *25*, 609−612.
(5) Jonsson, J.; Lindeke, B. *Acta Pharm. Suec.* **1976**, *13*, 313−320.
(6) Franklin, M. R. *Mol. Pharmacol.* **1974**, *10*, 975−985.
(7) Hirata, M.; Lindeke, B.; Orrenius, S. *Biochem. Pharmacol.* **1979**, *28*, 479−484.
(8) Hirota, K.; Itano, H. A. *J. Biol. Chem.* **1978**, *253*, 3477−3481.
(9) Mansuy, D.; Chottard, J. C.; Chottard, G. *Eur. J. Biochem.* **1977**, *76*, 617−623.
(10) Keilin, D.; Hartree, E. F. *Nature* **1943**, *151*, 390−391.
(11) Murayama, M. *J. Biol. Chem.* **1960**, *235*, 1024−1028.
(12) Gibson, Q. H. *Biochem. J.* **1960**, *77*, 519−526.
(13) Stone, J. R.; Marletta, M. A. *Biochemistry* **1995**, *34*, 16397−16403.
(14) *The Chemistry of Functional Groups: The Chemistry of Amino, Nitroso and Nitro Compounds and Their Derivatives*; Patai, S., Ed.; John Wiley and Sons: Chichester, U.K., 1996; Supplement F2.
(15) *The Chemistry of Functional Groups: The Chemistry of Amino, Nitroso and Nitro Compounds and Their Derivatives;* Patai, S., Ed.; John Wiley and Sons: Chichester, U.K., 1982; Supplement F.
(16) *The Chemistry of Functional Groups: The Chemistry of the Nitro and Nitroso Groups*; Feuer, H., Ed.; Interscience: New York, 1969.
(17) Williams, D. L. H. *Nitrosation*; Cambridge University Press: Cambridge, U.K., 1988.
(18) Zuman, P.; Shah, B. *Chem. Rev.* **1994**, *94*, 1621−1641.
(19) Park, J.; Dyakov, I. V.; Mebel, A. M.; Lin, M. C. *J. Phys. Chem. A* **1997**, *101*, 6043−6047 and references therein.
(20) Glaser, R.; Murmann, R. K.; Barnes, C. L. *J. Org. Chem.* **1996**, *61*, 1047−1058 and references therein.
(21) Reents, W. D., Jr.; Freiser, B. S. *J. Am. Chem. Soc.* **1980**, *102*, 271−276.
(22) Cacace, F.; Ricci, A. *Chem. Phys. Lett.* **1996**, *253*, 184−188 and references therein.
(23) Cameron, M.; Gowenlock, B. G.; Vasapollo, G. *Chem. Soc. Rev.* **1990**, *19*, 355−379.

Chart 1
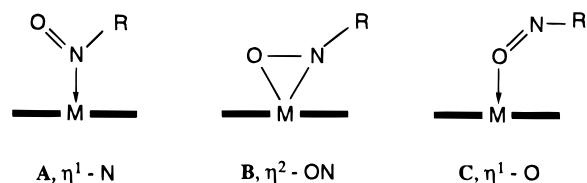
form appear to be limited to Rh[33] and Hf,[34] whereas the μ-η^1: η^2 form is known for a trimetallic Os cluster.[35] Structurally characterized examples of type **C** complexes are also rare and are so far only established for Mn,[36] Fe,[37] Sn,[38] and Zn.[39]

We are interested in the coordination chemistry of ArNO compounds with the group 8 metalloporphyrins as synthetic heme models. We recently reported *N*-binding and *O*-binding of ArNO to ferrous and ferric porphyrins, respectively.[37] James and co-workers have isolated and spectroscopically characterized PhNO complexes of ruthenium porphyrins.[40] Iron phthalocyanine complexes containing ArNO ligands are also known.[41] To the best of our knowledge, however, no monometallic osmium complexes containing *C*-nitroso ligands have been reported.

In this paper, we report the synthesis and spectroscopic characterization of a number of osmium nitrosoarene porphyrin complexes. Their solid-state molecular and crystal structures have been determined by single-crystal X-ray diffraction.

Experimental Section

All reactions were performed under an atmosphere of prepurified nitrogen using standard Schlenk techniques and/or in an Innovative Technology Labmaster 100 drybox unless stated otherwise. Solvents were distilled from appropriate drying agents under nitrogen just prior to use: CH_2Cl_2 (CaH$_2$), hexane (Na/benzophenone/tetraglyme), and toluene (Na).

Chemicals. (TTP)Os(CO), (TPP)Os(CO), and (OEP)Os(CO) were prepared by literature methods (TTP = 5,10,15,20-tetra-*p*-tolylporphyrinato dianion, TPP = 5,10,15,20-tetraphenylporphyrinato dianion, OEP = 2,3,7,8,12,13,17,18-octaethylporphyrinato dianion, TMP = 5,10,

15,20-tetramesitylporphyrinato dianion).[42] PhNO (97%) and *o*-tolNO (97%) were purchased from Aldrich Chemical Co. and used as received. Chloroform-*d* (99.8%) and toluene-*d*$_8$ (99.6%) were obtained from Cambridge Isotope Laboratories, subjected to three freeze−pump−thaw cycles, and stored over Linde 4 Å molecular sieves. Elemental analyses were performed by Atlantic Microlab, Norcross, GA.

Instrumentation. Infrared spectra were recorded on a Bio-Rad FT-155 FTIR spectrometer. ^{1}H NMR spectra were obtained on either a Varian XL-300 or a Varian XL-400 spectrometer, and the signals (in ppm) were referenced to the residual signals of the solvents employed. All coupling constants are in Hz. FAB mass spectra were obtained on a VG-ZAB-E mass spectrometer. UV−vis spectra were recorded on a Hewlett-Packard model 8453 diode array instrument.

Preparation of (TTP)Os(PhNO)₂. Method I. To a toluene (20 mL) solution of (TTP)Os(CO) (0.040 g, 0.045 mmol) was added excess PhNO (0.011 g, 0.10 mmol). The solution was heated to reflux for 30 min, whereby the color of the solution changed from orange-red to brown (the reaction takes 5−6 h at room temperature). The volume of the solution was reduced to ca. 2 mL. The product was precipitated by adding hexane (4 mL) to the solution and keeping the mixture at ca −20 °C overnight. The supernatant solution was discarded, and the purple-brown crystalline solid was dried in vacuo for 3 h to give (TTP)-Os(PhNO)₂ (0.030 g, 0.028 mmol, 62% yield). Anal. Calcd for $C_{60}H_{46}O_2N_6Os$: C, 67.15; H, 4.32; N, 7.83. Found: C, 67.69; H, 4.78; N, 7.39. IR (KBr, cm^{-1}): ν_{NO} = 1291 s; also 3022 vw, 2917 vw, 1570 w, 1527 w, 1512 w, 1496 w, 1451 w, 1350 w, 1312 s, 1212 w, 1180 m, 1150 vw, 1107 w, 1071 w, 1014 s, 868 m, 831 w, 797 s, 766 m, 730 vw, 717 m, 691 m, 670 w, 662 w, 632 w, 524 m. ^{1}H NMR (CDCl$_3$, δ): 8.48 (s, 8H, *pyr*-H of TTP), 7.96 (d, *J* = 8, 8H, *o*-H of TTP), 7.50 (d, *J* = 8, 8H, *m*-H of TTP), 6.40 (t, *J* = 8, 2H, *p*-H of PhNO), 5.92 (t, *J* = 8, 4H, *m*-H of PhNO), 2.67 (s, 12H, C*H*$_3$ of TTP), 2.43 (d, *J* = 8, 4H, *o*-H of PhNO). Low-resolution mass spectrum (FAB): *m/z* 967 [(TTP)Os(PhNO)]$^+$ (14%), 860 [(TTP)Os]$^+$ (24%), 107 [PhNO]$^+$ (21%). UV−vis spectrum (λ (ϵ, mM^{-1} cm^{-1}), 8.40 × 10^{-6} M in CH$_2$Cl$_2$): 314 (29), 408 (136), 655 (6) nm.

Method II. To a CH$_2$Cl$_2$ (15 mL) solution of (TTP)Os(CO) (0.047 g, 0.053 mmol) was added PhNO (0.007 g, 0.065 mmol). The color of the solution changed from orange-red to a dirty dark brown. The mixture was left to stir for 20 min, and the volume of the solution was reduced to ca. 2 mL. The product mixture was precipitated by adding hexane (4 mL) and keeping the mixture at ca. −20 °C overnight. The supernatant was discarded, and the solid was dried in vacuo for 3 h to give a mixture of (TTP)Os(PhNO)₂ (major) and (TTP)-Os(CO)(PhNO) (minor) in a 3:1 ratio. The IR spectrum of the mixture (as a KBr pellet) contained a peak at 1972 cm^{-1} attributed to ν_{CO} of (TTP)Os(CO)(PhNO). Low-resolution mass spectrum (FAB) of mixture: *m/z* 967 [(TTP)Os(PhNO)]$^+$ (22%), 888 [(TTP)Os(CO)]$^+$ (14%), 860 [(TTP)Os]$^+$ (40%), 107 [PhNO]$^+$ (41%). Further reaction of this product mixture with PhNO in refluxing toluene produces (TTP)Os-(PhNO)₂ exclusively (0.023 g, 0.021 mmol, 40% overall yield from (TTP)Os(CO)).

Preparation of (TPP)Os(PhNO)₂. A procedure analogous to Method I above was used to synthesize purple (TPP)Os(PhNO)₂. No satisfactory elemental analysis was obtained in this case. IR (KBr, cm^{-1}): ν_{NO} = 1295 s; also 3054 vw, 3022 vw, 1597 w, 1575 w, 1530 w, 1506 w, 1489 w, 1478 w, 1450 sh, 1441 m, 1350 m, 1311 s, 1209 w, 1177 m, 1156 w, 1071 m, 1015 s, 1000 m, 920 w, 871 m, 832 w, 795 m, 767 m, 752 s, 735 w, 715 w, 701 s, 695 s, 666 m, 636 w, 527 w. Low-resolution mass spectrum (FAB): *m/z* 911 [(TPP)Os(PhNO)]$^+$ (11%), 804 [(TPP)Os]$^+$ (19%), 107 [PhNO]$^+$ (52%).

Preparation of (TMP)Os(PhNO)₂. To a toluene (20 mL) solution of (TMP)Os(CO) (0.058 g, 0.058 mmol) was added excess PhNO (0.020 g, 0.19 mmol). The mixture was heated to reflux for 25 min. The color of the solution turned from light red to light brown. All the solvent was then removed in vacuo. The product was filtered through a neutral alumina column in air with CH$_2$Cl$_2$ as eluent. The brown filtrate was taken to dryness, and the product was dried in vacuo for 5 h to give brown (TMP)Os(PhNO)₂ (0.052 g, 0.044 mmol, 76% yield).

(24) Mansuy, D.; Battioni, P.; Chottard, J.-C.; Riche, C.; Chiaroni, A. *J. Am. Chem. Soc.* **1983**, *105*, 455−463.

(25) Pilato, R. S.; McGettigan, C.; Geoffroy, G. L.; Rheingold, A. L.; Geib, S. J. *Oranometallics* **1990**, *9*, 312−317.

(26) Brouwer, E. B.; Legzdins, P.; Rettig, S. J.; Ross, K. J. *Organometallics* **1994**, *13*, 2088−2091.

(27) Pizzotti, M.; Porta, F.; Cenini, S.; Demartin, F.; Masciocchi, N. *J. Organomet. Chem.* **1987**, *330*, 265−278.

(28) Dutta, S. K.; McConville, D. B.; Youngs, W. J.; Chaudhury, M. *Inorg. Chem.* **1997**, *36*, 2517−2522.

(29) Ridouane, F.; Sanchez, J.; Arzoumanian, H.; Pierrot, M. *Acta Crystallogr.* **1990**, *C46*, 1407−1410.

(30) Liebeskind, L. S.; Sharpless, K. B.; Wilson, R. D.; Ibers, J. A. *J. Am. Chem. Soc.* **1978**, *100*, 7061−7063.

(31) Skoog, S. J.; Gladfelter, W. L. *J. Am. Chem. Soc.* **1997**, *119*, 11049−11060.

(32) Skoog, S. J.; Campbell, J. P.; Gladfelter, W. L. *Organometallics* **1994**, *13*, 4137−4139.

(33) Hoard, D. W.; Sharp, P. R. *Inorg. Chem.* **1993**, *32*, 612−620.

(34) Scott, M. J.; Lippard, S. J. *Organometallics* **1998**, *17*, 466−474.

(35) Ang, H. G.; Kwik, W. L.; Ong, K. K. *J. Fluorine Chem.* **1993**, *60*, 43−48.

(36) Fox, S. J.; Chen, L.; Khan, M. A.; Richter-Addo, G. B. *Inorg. Chem.* **1998**, *36*, 6465−6467.

(37) Wang, L.-S.; Chen, L.; Khan, M. A.; Richter-Addo, G. B. *Chem. Commun.* **1996**, 323−324.

(38) Matsubayashi, G.-E.; Nakatsu, K. *Inorg. Chim. Acta* **1982**, *64*, L163−L164.

(39) Hu, S.; Thompson, D. M.; Ikekwere, P. O.; Barton, R. J.; Johnson, K. E.; Robertson, B. E. *Inorg. Chem.* **1989**, *28*, 4552−4554.

(40) Crotti, C.; Sishta, C.; Pacheco, A.; James, B. R. *Inorg. Chim. Acta* **1988**, *141*, 13−15.

(41) Watkins, J. J.; Balch, A. L. *Inorg. Chem.* **1975**, *14*, 2720−2723.

(42) Che, C.-M.; Poon, C.-K.; Chung, W.-C.; Gray, H. B. *Inorg. Chem.* **1985**, *24*, 1277−1278.

Anal. Calcd for $C_{68}H_{62}O_2N_6Os$: C, 68.90; H, 5.27; N, 7.09. Found: C, 68.39; H, 5.50; N, 6.75. IR (KBr, cm^{-1}): ν_{NO} = 1276 s; also 2917 vw, 2850 vw, 1610 vw, 1586 vw, 1525 vw, 1478 w, 1452 w, 1436 m, 1380 w, 1344 w, 1324 w, 1310 w, 1206 w, 1181 w, 1155 w, 1063 m, 1015 s, 919 m, 868 m, 853 w, 833 m, 797 m, 765 w, 730 s, 720 s, 686 m, 671 w, 644 w, 635 w, 561 w. ^{1}H NMR (CDCl$_3$, δ): 8.26 (s, 8H, *pyr*-H of TMP), 7.20 (s, 8H, *m*-H of TMP), 6.29 (t, *J* = 8, 2H, *p*-H of PhNO), 5.81 (t, *J* = 8, 4H, *m*-H of PhNO), 2.79 (d, *J* = 8, 4H, *o*-H of PhNO), 2.56 (s, 12H, *p*-C*H₃* of TMP), 1.86 (s, 24H, *o*-C*H₃* of TMP). Low-resolution mass spectrum (FAB): *m/z* 1080 [(TMP)Os(PhNO) + H]$^+$ (3%), 972 [(TMP)Os]$^+$ (4%). UV–vis spectrum (λ (ϵ, mM^{-1} cm^{-1}), 3.72 × 10^{-6} M in CH$_2$Cl$_2$): 315 (42), 408 (163), 658 (10) nm.

Preparation of (OEP)Os(PhNO)₂. Purple-black (OEP)Os(PhNO)₂ was prepared by a procedure similar to that for (TMP)Os(PhNO)₂ in 45% isolated yield. Anal. Calcd for $C_{48}H_{54}O_2N_6Os$: C, 61.52; H, 5.81; N, 8.97. Found: C, 61.35; H, 5.87; N, 8.92. IR (KBr, cm^{-1}): ν_{NO} = 1286 s; also 2964 w, 2932 w, 2864 w, 1588 w, 1468 w, 1451 w, 1447 w, 1378 w br, 1304 m, 1231 w, 1177 w, 1152 m, 1112 w, 1057 m, 1019 m, 993 m, 960 m, 870 w, 840 w, 766 m, 747 w, 738 w, 718 w, 689 m, 670 w, 666 w, 657 w, 625 w. ^{1}H NMR (CDCl$_3$, δ): 9.93 (s, 4H, *meso*-H of OEP), 6.18 (t, *J* = 8, 2H, *p*-H of PhNO), 5.68 (t, *J* = 8, 4H, *m*-H of PhNO), 3.99 (q, *J* = 8, 16H, CH$_3$*CH₂* of OEP), 1.99 (d, *J* = 8, 4H, *o*-H of PhNO), 1.83 (t, *J* = 8, 24H, C*H₃*CH₂ of OEP). Low-resolution mass spectrum (FAB): *m/z* 938 [(OEP)Os(PhNO)₂]$^+$ (3%), 831 [(OEP)Os(PhNO)]$^+$ (22%), 724 [(OEP)Os]$^+$ (56%), 107 [PhNO]$^+$ (20%). UV–vis spectrum (λ (ϵ, mM^{-1} cm^{-1}), 5.93 × 10^{-6} M in CH$_2$Cl$_2$): 328 (sh, 41), 377 (124), 498 (26), 658 (9) nm.

Preparation of (OEP)Os(*o*-tolNO)₂. Black (OEP)Os(*o*-tolNO)₂ was prepared by procedures similar to those for (OEP)Os(PhNO)₂ and (TMP)Os(PhNO)₂ in 49% isolated yield. Anal. Calcd for $C_{50}H_{58}O_2N_6$-Os: C, 62.22; H, 6.06; N, 8.71. Found: C, 62.30; H, 6.06; N, 8.62. IR (KBr, cm^{-1}): ν_{NO} = 1290 s; also 2963 w, 2931 w, 2868 w, 1480 w, 1468 w, 1464 w, 1447 m, 1379 w, 1317 m, 1274 s, 1231 w, 1152 m, 1111 w, 1056 m, 1018 m, 992 m, 959 m, 886 m, 868 w, 859 w, 839 m, 749 s, 738 w, 718 m, 706 w, 664 w, 648 w, 626 w. ^{1}H NMR (toluene-d_8, δ): 10.02 (s, 4H, *meso*-H of OEP), 5.81 (app t, *J* = 7/8, 2H, *p*-H of *o*-tolNO), 5.45 (app t, *J* = 8/8, 2H, *m*-H of *o*-tolNO), 5.31 (d, *J* = 7, 2H, *m'*-H of *o*-tolNO), 3.91 (q, *J* = 7, 16H, CH$_3$*CH₂* of OEP), 1.82 (t, *J* = 7, 24H, C*H₃*CH₂ of OEP), 1.51 (d, *J* = 8, 2H, *o*-H of *o*-tolNO), −1.26 (s, 6H, C*H₃* of *o*-tolNO). ^{1}H NMR (CDCl$_3$, δ): 9.91 (s, 4H, *meso*-H of OEP), 5.99 (app t, *J* = 7/8, 2H, *p*-H of *o*-tolNO), 5.49 (app t, *J* = 7/8, 4H, *m*-H of *o*-tolNO), 3.99 (q, *J* = 8, 16H, CH$_3$*CH₂* of OEP), 1.82 (t, *J* = 8, 24H, C*H₃*CH₂ of OEP), 1.19 (d, *J* = 8, 2H, *o*-H of *o*-tolNO), −1.46 (s, 6H, C*H₃* of *o*-tolNO). Low-resolution mass spectrum (FAB): *m/z* 845 [(OEP)Os(*o*-tolNO)]$^+$ (3%), 724 [(OEP)-Os]$^+$ (49%), 121 [*o*-tolNO]$^+$ (6%). UV–vis spectrum (λ (ϵ, mM^{-1} cm^{-1}), 1.62 × 10^{-5} M in CH$_2$Cl$_2$): 322 (sh, 28), 383 (76), 499 (18) nm.

X-ray Structure Determinations. All the data sets were collected at low temperature using Mo Kα (λ = 0.710 73 Å) radiation. The data were corrected for Lorentz and polarization effects, and an empirical absorption correction[43a,b] based on ψ-scans was applied. All the structures were solved by the direct methods using the SHELXTL (Siemens) system[43b] and refined by full-matrix least-squares procedures on F^2 using all reflections. Hydrogen atoms were included with idealized parameters. See Table 1 for details.

(i) (TPP)Os(PhNO)₂. Although we were not successful in obtaining an analytically pure bulk sample, we were able to grow a suitable crystal from CH$_2$Cl$_2$/hexane at −20 °C. Data collection and structure solution were conducted at the University of Oklahoma. In addition to the molecule of (TPP)Os(PhNO)₂, the asymmetric unit also contains two CH$_2$Cl$_2$ solvent molecules. Two of the phenyl rings of (TPP)Os(PhNO)₂ (C27−C32 and C45−C50) appear to be slightly disordered and display large thermal motions. Figure 3 shows the molecule with 50% thermal ellipsoids.

(43) (a) Sheldrick, G. M. *SADABS. Program for Empirical Absorption Correction of Area Detector Data*; University of Göttingen: Göttingen, Germany, 1996. (b) Sheldrick, G. M. *SHELXTL Version 5 Reference Manual*; Bruker AXS: Madison, WI, 1994. (c) Spek, A. L. *Acta Crystallogr.* **1990**, *A46*, C34.

(ii) (TTP)Os(PhNO)₂. A suitable crystal was grown from a toluene/hexane mixture at ca. −20 °C. Data collection and structure solution were conducted at the University of Minnesota. Two half-hexane solvent molecules were ordered and are refined as anisotropic groups. PLATON[43c] identified an additional void which presumably contains disordered solvent. The potential solvent volume is 250.9 Å^3 in the unit cell volume of 2868.5 Å^3, or 8.7% of the whole. The total (positive) electron count/cell is 47.4, and the residual *R* improved about 0.7% when the corrected data were used for refinement. This void could possibly contain another hexane molecule, but that is speculative. Thus, the formula weight, empirical formula, absorption correction, and *F*(000) should be treated with caution. Atoms N2 and C19 were restrained to refine positive-definite, because these were slightly nonpositive definite otherwise. The tolyl group C28−C33 is disordered over two rotationally related sites. In the packing diagram, it is clear that it lies close to an inversion center, and both orientations are required simultaneously; otherwise bumping would occur. SHELXTL SAME restraints were applied to the fragments of this tolyl group and the *n*-hexane to impose reasonable distance restraints. Figure 2 shows the molecule with 50% thermal ellipsoids.

(iii) (TTP)Os(CO)(PhNO). A suitable crystal was adventitiously grown from a reaction mixture of (TTP)Os(CO) and crude *N,N*-dimethyl-4-nitrosoaniline (97%) which had been kept at −20 °C for 30 days. Data collection and structure solution were conducted at the University of Minnesota. The molecule has a crystallographically imposed center of symmetry, with the Os atom situated at the inversion center. The asymmetric unit contains only half of the unique molecule, and the other half is related by the inversion center. Both the CO and the ON(C₆H₅) ligands are disordered at the two axial sites, and they were refined with 50% occupancy. Figure 1 shows the structure with 20% thermal ellipsoids.

(iv) (TMP)Os(PhNO)₂. A suitable crystal was grown by slow solvent evaporation under inert atmosphere. Data collection and structure solution were conducted at the University of Wisconsin. Restraints were needed to refine the geometry of the solvent and the displacement parameters of the solvent and the aromatic ring attached to N5. Figure 4 shows the molecule with 50% thermal ellipsoids.

(v) (OEP)Os(*o*-tolNO)₂. A suitable crystal was grown by slow evaporation of the toluene-d_8 mixture of the reaction of (OEP)Os-(PhNO)₂ with excess *o*-tolNO (NMR tube reaction). Data collection and structure solution were conducted at the University of Oklahoma. The molecule has a crystallographically imposed center of symmetry with the Os atom situated at the inversion center. The asymmetric unit contains only half of the unique molecule, and the other half is related by the inversion center. The ON−tol group is completely disordered at two sites, and both fragments were refined with 50% occupancy. Figure 5 shows the molecule with 50% thermal ellipsoids (only one of the disordered ON−tol groups is shown for the sake of clarity).

Results and Discussion

The reactions of the (por)Os(CO) compounds with PhNO are summarized in Scheme 1. The (por)Os(PhNO)₂ products are moderately air-stable, showing no signs of decomposition in air after several months in the solid state and at least 24 h in solution. They are readily soluble in CH$_2$Cl$_2$. Some are also soluble in toluene (TTP, TMP) and benzene (TTP), moderately soluble in benzene (TPP), slightly soluble in hexane (TTP, OEP), or insoluble in hexane (TPP, TMP). The reaction of (TTP)-Os(CO) with 1 equiv of PhNO in CH$_2$Cl$_2$ at room temperature generates a 1:3 mixture of (TTP)Os(CO)(PhNO) (Figure 1) and (TTP)Os(PhNO)₂ (Figure 2) in ca. 40% isolated yield (and unreacted (TTP)Os(CO)). Importantly, the ν_{CO} of (TTP)Os(CO)-(PhNO) is at 1972 cm^{-1} (KBr), which is 56 cm^{-1} *higher* in energy than that of the precursor (TTP)Os(CO) (at 1916 cm^{-1}, KBr). Indeed, this observation is consistent with PhNO acting as a π-acid ligand toward the (TTP)Os(CO) fragment, thus making less electron density available for Os^{II}−CO back-

Table 1. Crystal Data and Structure Refinement

	(TPP)Os(PhNO)$_2$·2CH$_2$Cl$_2$	(TTP)Os(PhNO)$_2$·hexane	(TTP)Os(CO)(PhNO)·toluene
empirical formula (fw)	C$_{58}$H$_{42}$Cl$_4$N$_6$O$_2$Os (1186.98)	C$_{66}$H$_{60}$N$_6$O$_2$Os (1159.40)	C$_{62}$H$_{49}$N$_5$O$_2$Os (1086.26)
T, K	188(2)	173(2)	173(2)
diffractometer	Siemens P4	Siemens SMART Platform CCD	Siemens SMART Platform CCD
crystal system	triclinic	triclinic	triclinic
space group	$P\bar{1}$	$P\bar{1}$	$P\bar{1}$
unit cell dimensions	$a = 13.153(2)$ Å,	$a = 10.0066(3)$ Å,	$a = 11.2385(1)$ Å,
	$b = 14.663(2)$ Å,	$b = 11.2628(3)$ Å,	$b = 11.3499(2)$ Å,
	$c = 15.642(2)$ Å,	$c = 26.0574(6)$ Å,	$c = 11.9235(2)$ Å,
	$\alpha = 65.000(10)°$,	$\alpha = 83.362(1)°$,	$\alpha = 74.061(1)°$,
	$\beta = 68.355(6)°$,	$\beta = 83.171(1)°$,	$\beta = 67.810(1)°$,
	$\gamma = 73.332(9)°$	$\gamma = 81.368(1)°$	$\gamma = 85.073(1)°$
V, Z	2510.4(6) Å^3, 2	2868.54(13) Å^3, 2	1353.86(4) Å^3, 1
D(calcd), g/cm^3	1.570	1.342	1.332
abs coeff, mm^{-1}	2.803	2.271	2.401
$F(000)$	1184	1180	548
crystal size, mm	0.64 × 0.42 × 0.38	0.20 × 0.18 × 0.12	0.30 × 0.28 × 0.08
θ range for data collcn, deg	2.11−26.00	0.79−25.12	1.87−24.97
index ranges	$0 \leq h \leq 16$,	$-11 \leq h \leq 11$,	$-12 \leq h \leq 13$,
	$-16 \leq k \leq 16$,	$-13 \leq k \leq 13$,	$-12 \leq k \leq 13$,
	$-17 \leq l \leq 19$	$0 \leq l \leq 30$	$0 \leq l \leq 14$
no. of reflns collected	9808	14 385	8088
no. of indep reflns	9374 [$R_{int} = 0.0366$]	9721 [$R_{int} = 0.0584$]	4665 [$R_{int} = 0.0397$]
data/restraints/parameters	9340/46/641	9717/33/718	4665/69/355
goodness-of-fit on F^2	1.063	1.048	1.047
obsd no. of reflns [$I > 2\sigma(I)$]^{a,b}	8516	6852	4185
final R indices [$I > 2\sigma(I)$]^{a,b}	R1 = 0.0334, wR2 = 0.0795	R1 = 0.0919, wR2 = 0.2037	R1 = 0.0728, wR2 = 0.1790
R indices (all data)^{a,b}	R1 = 0.0399, wR2 = 0.0940	R1 = 0.1230, wR2 = 0.2264	R1 = 0.0791, wR2 = 0.1864
largest diff peak and hole, e Å^{-3}	1.234 and −1.136	4.562 and −3.235	2.316 and −1.193

	(TMP)Os(PhNO)$_2$·benzene	(OEP)Os(o-tolNO)$_2$
empirical formula (fw)	C$_{74}$H$_{68}$N$_6$O$_2$Os (1263.54)	C$_{50}$H$_{58}$N$_6$O$_2$Os (965.22)
T, K	133(2)	188(2)
diffractometer	Siemens P4/CCD	Siemens P4
crystal system	monoclinic	monoclinic
space group	$P2_1/n$	$P2_1/c$
unit cell dimensions	$a = 17.3716(3)$ Å,	$a = 8.759(1)$ Å,
	$b = 20.0394(3)$ Å,	$b = 12.370(2)$ Å,
	$c = 19.8667(2)$ Å,	$c = 19.786(2)$ Å,
	$\alpha = 90°$,	$\alpha = 90°$,
	$\beta = 112.070(2)°$,	$\beta = 93.42(1)°$,
	$\gamma = 90°$	$\gamma = 90°$
V, Z	6409.2(2) Å^3, 4	2140.0(5) Å^3, 2
D(calcd), g/cm^3	1.309	1.498
abs coeff, mm^{-1}	2.039	3.027
$F(000)$	2584	984
crystal size, mm	0.54 × 0.42 × 0.02	0.28 × 0.44 × 0.32
θ range for data collcn, deg	1.50−28.06	1.94−25.00
index ranges	$-22 \leq h \leq 19$,	$0 \leq h \leq 10$,
	$0 \leq k \leq 25$,	$0 \leq k \leq 14$,
	$0 \leq l \leq 26$	$-23 \leq l \leq 23$
no. of reflns collected	25 616	4028
no. of indep reflns	11904 [$R_{int} = 0.0776$]	3763 [$R_{int} = 0.0594$]
data/restraints/parameters	11897/109/749	3643/629/349
goodness-of-fit on F^2	1.256	1.503
obsd no. of reflns [$I > 2\sigma(I)$]^{a,b}	6986	2704
final R indices [$I > 2\sigma(I)$]^{a,b}	R1 = 0.0831, wR2 = 0.2056	R1 = 0.0507, wR2 = 0.1324
R indices (all data)^{a,b}	R1 = 0.1507, wR2 = 0.2439	R1 = 0.0821, wR2 = 0.2196
largest diff peak and hole, e Å^{-3}	5.328 and −2.469	2.124 and −1.359

^{a} R1 = $\sum||F_o| - |F_c||/\sum|F_o|$. ^{b} wR2 = $\{\sum[w(F_o^2 - F_c^2)^2]/\sum[wF_o^4]\}^{1/2}$.

donation, thereby raising ν_{CO}. For comparison, the coordination of Lewis bases to (por)Os(CO) compounds generally results in a lowering of ν_{CO} in the (por)Os(CO)(L) derivatives.[44] When this mixture and excess PhNO are dissolved in toluene and the solution is heated to reflux, quantitative conversion to the (TTP)-Os(PhNO)$_2$ product occurs. Interestingly, IR monitoring (of ν_{CO}) of the reactions of (por)Os(CO) with 1 equiv of PhNO in CH$_2$Cl$_2$ reveals similar formations of the respective (por)Os-

(CO)(PhNO) intermediates for the TTP (1968 cm^{-1}; $\Delta\nu_{CO}$ = +74 cm^{-1}), TMP (1966 cm^{-1}; $\Delta\nu_{CO}$ = +63 cm^{-1}), and OEP (1958 cm^{-1}; $\Delta\nu_{CO}$ = +72 cm^{-1}) analogues.

All the above-mentioned (por)Os(PhNO)$_2$ products are obtained by the direct reaction of (por)Os(CO) with excess PhNO in refluxing toluene. The molecular structures of (TPP)Os-(PhNO)$_2$ and (TMP)Os(PhNO)$_2$ are shown in Figures 3 and 4, respectively, and will be discussed later. The (OEP)Os(o-tolNO)$_2$ compound (Figure 5) is prepared similarly from (OEP)-Os(CO) and excess o-tolNO in 49% yield. It is also obtained

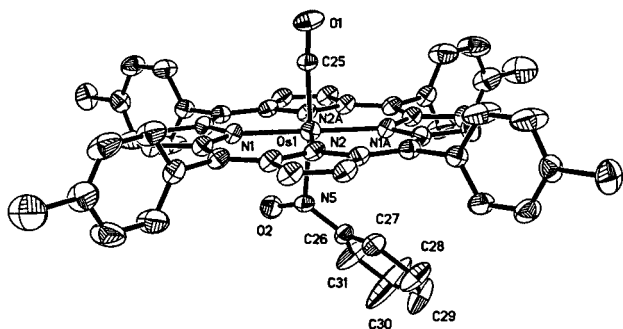(44) Buchler, J. W.; Kokisch, W.; Smith, P. D. *Struct. Bonding* **1978**, *34*, 79−134.

Figure 1. Molecular structure of (TTP)Os(CO)(PhNO). The CO and PhNO ligands are disordered over the two axial sites; however, only one of these disordered arrangements is shown. Hydrogen atoms have been omitted for clarity.
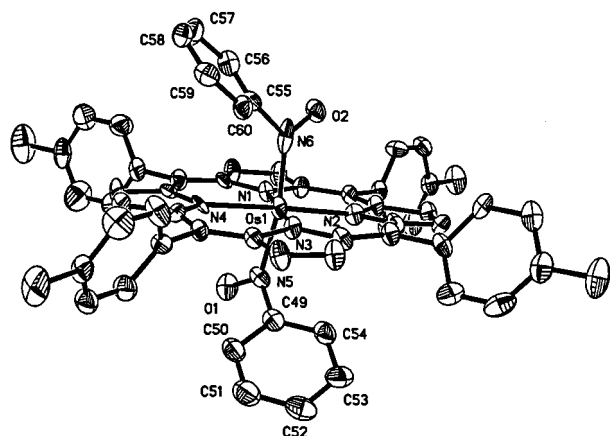

Figure 3. Molecular structure of (TPP)Os(PhNO)$_2$. Hydrogen atoms have been omitted for clarity.
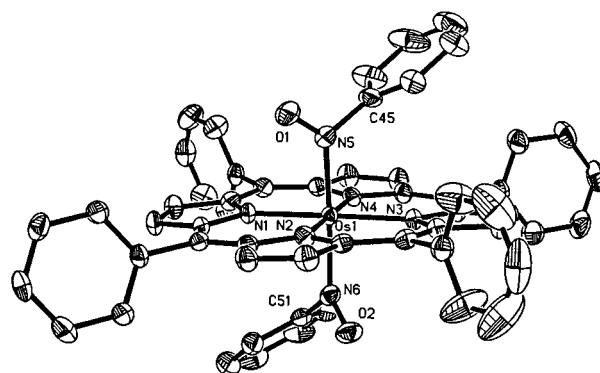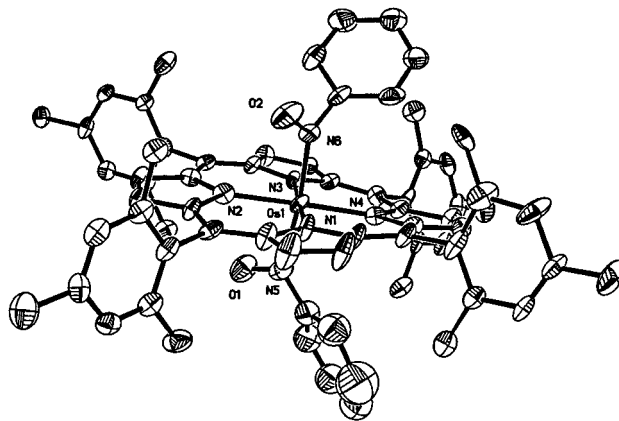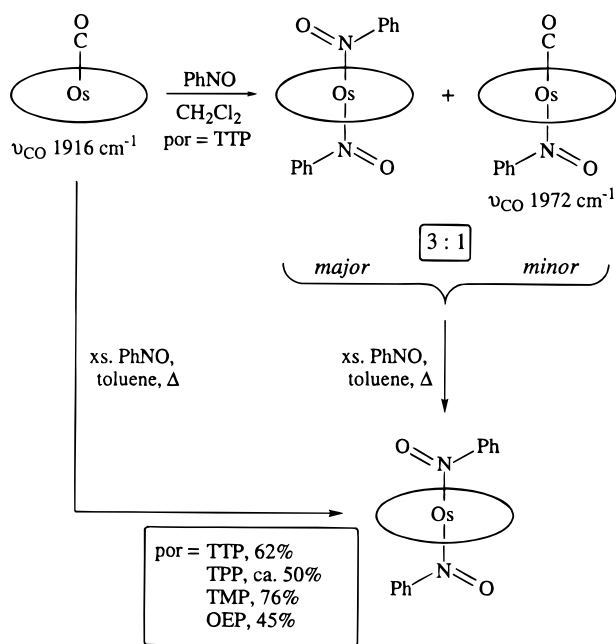

Figure 2. Molecular structure of (TTP)Os(PhNO)$_2$. Hydrogen atoms have been omitted for clarity.

Figure 4. Molecular structure of (TMP)Os(PhNO)$_2$. Hydrogen atoms have been omitted for clarity.

Scheme 1

The peak at -1.26 ppm is assigned to the methyl resonance of the *o*-tolNO group in (OEP)Os(*o*-tolNO)$_2$ (confirmed by the ^{1}H NMR spectrum of an authentic sample). Hence, we attribute the peak at -1.15 ppm to the methyl resonance of the presumed (OEP)Os(*o*-tolNO)(PhNO) intermediate.

Bubbling CO through a CH$_2$Cl$_2$ solution of (TMP)Os(PhNO)$_2$ for 35 min at room temperature does not result in PhNO displacement; the bis(nitrosobenzene) complex remains intact (as judged by IR, ^{1}H NMR, and UV−vis spectroscopy).

Spectroscopic Characterization. The IR spectra of the (por)Os(PhNO)$_2$ compounds show bands due to both the porphyrin macrocycles[45] as well as the PhNO ligands. A noticeable new band occurs in the 1295−1276 cm^{-1} range (other bands may be obscured by the porphyrin bands) and is attributed to the ν_{NO} of the coordinated PhNO groups. This band is shifted to lower energy from that of PhNO vapor at 1523 cm^{-1}.[46,47] The use of Ph^{15}NO in the reaction to produce (OEP)Os(PhNO)$_2$ shifts the 1286 cm^{-1} band to 1266 cm^{-1} ($\Delta\nu_{NO} = -20$ cm^{-1}), consistent with our assignment of this band to ν_{NO}.[48] The ν_{NO} values in the (por)Os(PhNO)$_2$ compounds decrease slightly in the order TPP (1295 cm^{-1}) > TTP (1291 cm^{-1}) > OEP (1286 cm^{-1}), and this feature is consistent with the order of increased

from the ligand exchange reaction of (OEP)Os(PhNO)$_2$ with *o*-tolNO. For example, when a 1:6 mixture of (OEP)Os(PhNO)$_2$ and *o*-tolNO is made up in toluene-d_8 and the reaction monitored by ^{1}H NMR spectroscopy, no reaction is found to occur over a 30 min period at room temperature. When the mixture is heated to 50 °C, however, two new peaks at -1.15 and -1.26 ppm are observed to form in a 1:1.3 equilibrium ratio after 20 min.

(45) Kitagawa, T.; Ozaki, Y. *Struct. Bonding* **1987**, *64*, 71−114.
(46) Bradley, G. M.; Strauss, H. L. *J. Phys. Chem.* **1975**, *79*, 1953−1957.
(47) The ν_{NO} values of *C*-nitroso compounds generally fall in the 1488−1621 cm^{-1} range. See Chapter 3 of ref 16.
(48) Ph^{15}NO was prepared by the oxidation of Ph^{15}NH$_2$ (Cambridge Isotope Laboratories) with 3-chloroperbenzoic acid: Bleasdale, C.; Ellis, M. K.; Farmer, P. B.; Golding, B. T.; Handley, K. F.; Jones, P.; McFarlane, W. *J. Labeled Compd. Radiopharm.* **1993**, *33*, 739−746.
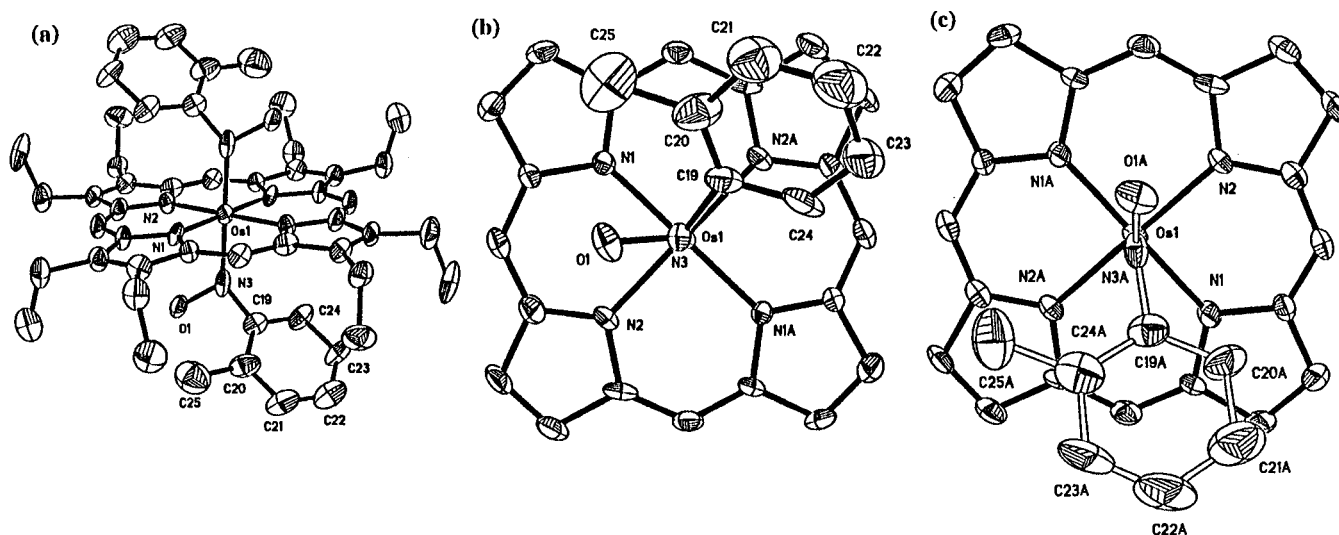
Figure 5. Molecular structure of (OEP)Os(*o*-tolNO)$_2$. (a) View showing only one set of the disordered *o*-tolNO groups and omitting hydrogen atoms for clarity. (b) View along the N3−Os1 bond, showing the orientation of the axial *o*-tolNO group with respect to the porphyrin skeleton. (c) View along the N3A−Os1 bond of the second disordered PhNO position. Selected bond lengths (Å) and angles (deg): Os1−N1 = 2.051(5), Os1−N2 = 2.068(5), Os1−N3 = 2.012(11), Os1−N3A = 1.985(10), N3−O1 = 1.273(13), N3A−O1A = 1.219(12); N3−Os1−N1 = 80.7(4), N3A−Os1−N1 = 94.3(3).

basicity of the porphyrin macrocycles,[49] which in turn results in increased back-bonding of electron density into the empty π^* orbitals of PhNO. For comparison, the ν_{NO}'s for the related (OEP)Ru(PhNO)$_2$[40] and (TPP)Fe(PhNO)$_2$[37] compounds are at 1339 and 1353 cm^{-1}, respectively, reflecting the stronger π-back-donation of electron density from Os to PhNO in these types of complexes.

The ^{1}H NMR spectra of the (por)Os(PhNO)$_2$ complexes consist of sharp peaks for the porphyrin macrocycle in the range normally associated with diamagnetic Os^{II} porphyrins. In addition, only one set of pyrrole H resonances are observed for the tetraarylporphyrin macrocycles (and one set of *meso*-H's are observed for OEP), and the trans PhNO groups are also rendered equivalent on the NMR time scale. The $\delta_{pyrrole}$ peak of (TMP)Os(PhNO)$_2$ is at 8.26 ppm, which is slightly upfield from that of (TTP)Os(PhNO)$_2$ at 8.48 ppm and is consistent with the increased basicity of the TMP macrocycle.[50] Furthermore, only one set of *o*- and *m*-H peaks of the tetraaryl substituents on the porphyrin rings are obtained for the (TTP)-Os(PhNO)$_2$ compound (and one set of *m*-H peaks for the TMP analog), suggesting axial symmetry in these complexes or fast rotation of the porphyrin aryl substituents on the NMR time scale.

Crystallographic Characterization. The molecular structures of the five (por)Os(ArNO)-containing complexes are shown in Figures 1−5. All the nitrosoarene ligands in these complexes are attached to the formally Os^{II} centers via an η^1-N bonding mode (**A** in Chart 1; see Introduction). Important structural parameters for the compounds are summarized in Figure 6. Perpendicular atom displacements of the atoms in the porphyrin skeleton from the 24-atom mean porphyrin plane are shown in the middle of Figure 6. The largest displacements are observed for (TMP)Os(PhNO)$_2$, which indicates the largest

deviation of the porphyrin plane from ideal planarity (Figure 6).

The Os−N(por) distances for the tetraaryl-substituted porphyrins lie in the 2.037(10)−2.107(9) Å range, and these are typical for such Os^{II} porphyrins.[51] The axial Os−N distances range from 1.931(13) Å in (TTP)Os(PhNO)$_2$ to 2.049(12) Å in the sterically encumbered (TMP)Os(PhNO)$_2$. However, the longest axial Os−N distance occurs in the carbonyl complex, namely (TTP)Os(CO)(PhNO), with a value of 2.18(2) Å. Although there are some slight differences in the trans axial Os−N distances within each (por)Os(PhNO)$_2$ complex in the solid state, these differences are not chemically significant, since both PhNO ligands are chemically and spectroscopically (IR and ^{1}H NMR) equivalent. Interestingly, the axial N−Os−N bond angles (involving both axial PhNO ligands) of 169.5(4)-174.59(14)° in the (por)Os(PhNO)$_2$ complexes deviate from strict linearity (bottom of Figure 6). However, such deviations have also been noted for some other group 8 metalloporphyrins such as (TTP)Os(CH$_2$SiMe$_3$)$_2$ (140(1)°)[53] and (TTP)Os(*p*-NC$_6$H$_4$NO$_2$)$_2$ (165.1(2)°).[54,55] The nitrosyl O−N bond lengths in the (por)Os−nitrosobenzene complexes are in the 1.249(4)−1.31(2) Å range and do not show a significant trend within these complexes. The O−N bond length for the nitrosobenzene dimer (*cis*-azobenzene dioxide) as determined by X-ray diffraction is 1.265(4) Å (average).[58]

(49) (a) Worthington, P.; Hambright, P.; Williams, R. F. X.; Reid, J.; Burnham, C.; Shamin, A.; Turay, J.; Bell, D. M.; Kirkland, R.; Little, R. G.; Datta-Gupta, N.; Eisner, U. *J. Inorg. Biochem.* **1980**, *12*, 281−291. (b) Kadish, K. M. *Prog. Inorg. Chem.* **1986**, *34*, 435−605.

(50) See ref 44 for an informative discussion of cis and trans effects/influences in transition metal porphyrins.

(51) See Table 3 and ref 32 of ref 52 for a listing of structurally characterized osmium porphyrins.

(52) Chen, L.; Khan, M. A.; Richter-Addo, G. B. *Inorg. Chem.* **1998**, *37*, 533−540.

(53) Leung, W.-H.; Hun, T. S. M.; Wong, K.-Y.; Wong, W.-T. *J. Chem. Soc., Dalton Trans.* **1994**, 2713−2718.

(54) Smieja, J. A.; Omberg, K. M.; Breneman, G. L. *Inorg. Chem.* **1994**, *33*, 614−616.

(55) Scheidt and co-workers recently reported high-quality X-ray crystal structures of the five-coordinate (OEP)Fe(NO)[56] and (OEP)Co(NO)[57] compounds which also show tilting of the "perpendicular" axial M−N(O) vectors.

(56) Ellison, M. K.; Scheidt, W. R. *J. Am. Chem. Soc.* **1997**, *119*, 7404−7405.

(57) Ellison, M. K.; Scheidt, W. R. *Inorg. Chem.* **1998**, *37*, 382−383.

(58) Dietrich, D. A.; Paul, I. C.; Curtin, D. Y. *J. Am. Chem. Soc.* **1974**, *96*, 6372−6380.
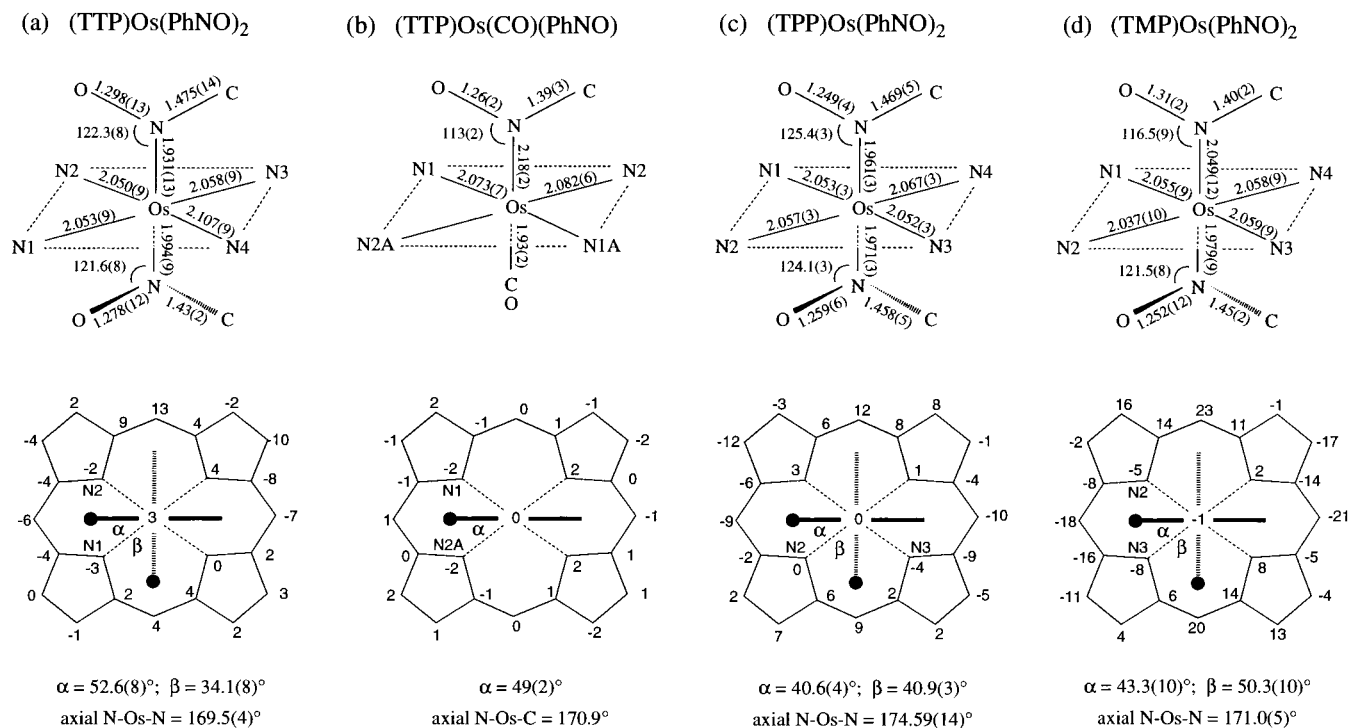
Figure 6. Structural data for the osmium nitrosobenzene complexes. Selected bond lengths and angles are shown at the top. Perpendicular atom displacements from the 24-atom porphyrin plane (in 0.01 Å units) are shown at the bottom. Also shown are the nitrosobenzene orientations: α and β are torsion angles involving $O-N-Os-N$(por). The solid dot represents the nitroso oxygen atom, the solid line represents the $O-N-C$ unit of the PhNO ligand situated above the plane, and the dashed line represents the equivalent group situated below the plane.

The PhNO ligands in the (por)Os(PhNO)$_2$ complexes are oriented perpendicular to each other and essentially bisect porphyrin nitrogens (middle of Figure 6), and this is consistent with this orientation enabling maximum π-back-bonding from the filled HOMO d_{xz} and d_{yz} orbitals of the formally d^6 (por)-Os^{II} fragment into the empty π^* orbitals of the PhNO ligands. We have observed a similar orientation in the related (TPP)-Fe(PhNO)$_2$ complex.[37] Similar axial ligand orientations have been observed for some group 8 metalloporphyrins [59–64] The structure of (OEP)Os(o-tolNO)$_2$ is shown in Figure 5. In this example, the nitrosoarene ligands are disordered, with N2−Os1-N3−O1 (Figure 5b) and N2−Os1-N3A-O1A (Figure 5c) torsion angles of −28(1) and 48(1)°, respectively. The sum of angles around the N3 and N3A atoms are very close to 360°, indicating planarity around these nitroso nitrogens.

The solid-state structure of (TTP)Os(CO)(PhNO) provides an interesting comparison with that of the related (TTP)Os(CO)-(Et$_2$NNO).[65] In the latter compound, the nitrosamine ligand is O-bound in an η^1-fashion to the osmium center. To the best of our knowledge, the only other (por)Os(CO)-containing structure to be reported is that of (OEPMe$_2$)Os(CO)(py) (Os−C = 1.828-(5) Å, C−O = 1.151(7) Å, Os−C−O = 178.9(14)°).[66] The Os−C bond length of 1.93(2) Å in (TTP)Os(CO)(PhNO) is *longer* than that in (TTP)Os(CO)(Et$_2$NNO) (1.818(11) Å), suggestive of *decreased* Os→CO back-bonding in (TTP)Os-(CO)(PhNO) relative to that in (TTP)Os(CO)(Et$_2$NNO). This view is consistent with the IR spectroscopic result discussed in the previous section, which suggested that the PhNO ligand acts as a π-acid in (TTP)Os(CO)(PhNO) (ν_{CO} = 1972 cm^{-1}, KBr), effectively withdrawing electron density from the osmium center. In contrast, however, the Et$_2$NNO ligand in (TTP)Os-(CO)(Et$_2$NNO) (ν_{CO} = 1902 cm^{-1}, KBr) behaves as an overall electron donor to the osmium center. However, the C−O bond length of 1.144(5) Å in (TTP)Os(CO)(PhNO) is similar to that in (TTP)Os(CO)(Et$_2$NNO) (1.140(12) Å). The Os−C−O bond in (TTP)Os(CO)(PhNO) is linear (175(4)°) and is similar to that in (TTP)Os(CO)(Et$_2$NNO) (177.9(10)°).

We were interested in determining the steric and electronic effects of altering the nature of the (por)Os fragment on the axial PhNO ligand orientations. We employed the sterically demanding TMP macrocycle to determine if the sterically enhanced *meso* positions of the TMP macrocycle would force an orientation of the PhNO ligands such that their nitroso fragments would eclipse the porphyrin nitrogens. As seen in the middle right section of Figure 6, the nature of the TMP macrocycle did not have a substantial effect on the orientation of the axial PhNO ligands in the (TMP)Os(PhNO)$_2$ complex. However, the TMP macrocycle was found to be the most distorted from ideal planarity. These observations imply that this binding orientation is largely determined by electronics rather than sterics. Selected structural data involving the metal−PhNO interactions are shown in Table 2.

As can be seen in this Table 2, there is no substantial difference in the angles that the projection of the nitrosobenzene N−C line makes with the 24-atom mean porphyrin planes

(59) Shokhirev, N. V.; Walker, F. A. *J. Am. Chem. Soc.* **1998**, *120*, 981−990.

(60) Raitsimring, A. M.; Walker, F. A. *J. Am. Chem. Soc.* **1998**, *120*, 991−1002.

(61) Safo, M. K.; Gupta, G. P.; Walker, F. A.; Scheidt, W. R. *J. Am. Chem. Soc.* **1991**, *113*, 5498−5510.

(62) Momot, K. I.; Walker, F. A. *J. Phys. Chem. A* **1997**, *101*, 9207−9216.
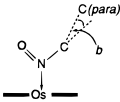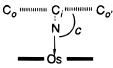
(63) Nasri, H.; Ellison, M. K.; Chen, S.; Huynh, B. H.; Scheidt, W. R. *J. Am. Chem. Soc.* **1997**, *119*, 6274−6283.

(64) Scheidt, W. R.; Lee, Y. J. *Struct. Bonding* **1987**, *64*, 1−70.

(65) Chen, L.; Yi, G.-B.; Wang, L.-S.; Dharmawardana, U. R.; Dart, A. C.; Khan, M. A.; Richter-Addo, G. B. *Inorg. Chem.* **1998**, *37*, 4677−4688.

(66) Buchler, J. W.; Lay, K. L.; Smith, P. D.; Scheidt, W. R.; Rupprecht, G. A.; Kenny, J. E. *J. Organomet. Chem.* **1976**, *110*, 109−120.

Table 2. Selected Structural Data (deg)

	a	b	c
(TTP)Os(CO)(PhNO)	50.4	4.4	50.2
(TTP)Os(PhNO)$_2$	54.6, 49.9	0.6, 2.3	61.3, 58.2
(TPP)Os(PhNO)$_2$	56.6, 56.3	1.4, 1.1	97.1, 78.1
(TMP)Os(PhNO)$_2$	40.1, 50.9	5.7, 4.6	43.1, 73.3
(OEP)Os(o-tol)$_2$	52.1, 58.8	3.8, 2.5	60.2, 98.7

[a] The angle between the projection of the N−C bond and the 24-atom mean porphyrin plane. [b] The angle made by the upward tilt of the C_{ipso}−C_{para} line (of PhNO) and the N−C bond. [c] The twist angle of the phenyl group (of PhNO) as measured by the angle between the axial Os−N−C_{ipso} plane and the C_{ortho}−C_{ipso}−$C_{ortho'}$ plane of the PhNO ligand.

(second column). However, the phenyl (of PhNO) tilt appears largest for the TMP complex (third column), presumably because of steric repulsion of the PhNO ligand by the *meso* mesityl groups of the TMP macrocycle. Not surprisingly, the twist angle of the phenyl group (of PhNO) as measured by the angle between the axial Os−N−C_{ipso} plane and the C_{ortho}−

C_{ipso}−$C_{ortho'}$ plane of the PhNO ligand is also largest for one of the PhNO groups in the sterically crowded TMP complex (fourth column, smallest angle of 43.1°).

Summary. We have prepared the first monometallic *C*-nitroso compounds of osmium. They have been fully characterized by spectroscopy and by single-crystal X-ray crystallography. Analyses of the solid-state structural data suggest that the nitrosoarene ligand orientation is dictated largely by electronics rather than sterics. Furthermore, the spectroscopic and structural data for (TTP)Os(CO)(PhNO) suggest that the PhNO ligand acts as a π-acceptor in these six-coordinate η^1-N complexes.

Supporting Information Available: Additional structural drawings and listings of crystal data, atomic coordinates, anisotropic displacement parameters, bond lengths and angles, hydrogen coordinates and isotropic displacement parameters, torsion angles, and least-squares planes (81 pages). Ordering information is given on any current masthead page.

IC980463U